Controlling instability and squeezing from a cascaded frequency doubler

K. V. Kheruntsyan, G. Yu. Kryuchkyan,* N. T. Mouradyan, and K. G. Petrosyan
Institute for Physical Research, National Academy of Sciences, Ashtarak-2, 378410, Armenia
(Received 22 July 1996; revised manuscript received 17 March 1997)

We present a semiclassical and quantum analysis of a nonlinear optical interaction in a cavity in which an externally driven fundamental mode at frequency ω transforms into the second-harmonic mode 2ω and then into the fourth-harmonic mode 4ω via cascaded frequency-doubling processes $\omega+\omega\rightarrow 2\omega$ and $2\omega+2\omega\rightarrow 4\omega$. In the adiabatic limit of the strongly damped fourth-harmonic mode the nonlinear system is equivalent to the process of intracavity second-harmonic generation combined with nonlinear two-photon absorption from the second-harmonic mode. Semiclassical steady states and linear stability analysis show that possible operation regimes are substantially different from those for the pure second-harmonic-generation process. It is shown in particular that the system is characterized by two critical points: Starting from a certain critical value of the driving field intensity, one observes self-pulsing instability; however, at higher intensities, beyond a second critical point, the system turns back to the stable generation regime. Moreover, under appropriate values of the control parameters, one may arrive at a complete quenching of self-pulsing behavior and at stabilization of the steady states in the entire domain of the driving field intensity. These stabilization properties become important when turning to the analysis of the quantum fluctuations and quadrature squeezing effect in the fundamental and second-harmonic modes within the ranges of linearized treatment of fluctuations. Due to the emergence of stability in the behavior of the system at high level of coherent excitation, the system becomes capable of generation of bright light with enhanced squeezing properties. [S1050-2947(97)08911-7]

PACS number(s): 42.65.−k

I. INTRODUCTION

Frequency doubling or second-harmonic generation (SHG) in a cavity is one of the basic processes in the field of nonlinear and quantum optics. It consists of a transformation, via a $\chi^{(2)}$-nonlinear crystal, of pairs of photons of an externally driven fundamental mode of the cavity with frequency ω into photons of the second-harmonic mode with frequency 2ω $(\omega+\omega\rightarrow 2\omega)$. A consistent theoretical analysis of the SHG, including quantum fluctuations and dissipation effects, has been presented in [1]. It was shown in particular that in the steady-state regime this nonlinear process is characterized by a certain critical point with respect to the driving field intensity, above which the system turns from the stable generation regime to the unstable regime. In the instability domain the intensities of the fundamental and second-harmonic modes demonstrate self-pulsing temporal behavior, which has been observed experimentally [2].

SHG was also one of the first processes that were considered for production of quadrature squeezed light [3,4]. Several experiments have been performed [5–7] that demonstrated squeezed noise reduction in both the fundamental and second-harmonic modes. We note that an attractive property of SHG is related to the fact that the squeezed light produced in this process is not the squeezed vacuum but an amplitude squeezed light with a nonzero coherent component. This property is of great importance when we look for a source of bright squeezed light, i.e., a squeezed light with a high level of coherent excitation. Recent experimental results on generation of bright squeezed light at the second-harmonic mode frequency are related to utilizing a singly resonant frequency-doubling scheme [8].

It should be pointed out, however, that in SHG there exist some limitations on the intensity and degree of squeezing of the fundamental and second-harmonic modes available in the stable steady-state regime. They originate from the instability appearing when the critical value of the driving field intensity is approached. As is known from theoretical considerations [4], the maximal degree of squeezing in the fundamental and second-harmonic modes is approached in the vicinity of the critical point. Hence the maximal intensities of the highly squeezed modes in the stable steady-state regime turn out to be limited by their critical values. Note also that although the squeezing in a generalized sense was shown to survive in the instability domain [9], our attention in this paper is directed toward the bright squeezing obtainable in the stable generation regime.

In the present paper we propose a nonlinear optical scheme that is capable of generating bright squeezed light with enhanced squeezing properties. It contains two cascaded nonlinear processes of frequency doubling, taking place inside the same cavity and transforming an externally driven fundamental mode ω into the second-harmonic mode 2ω $(\omega+\omega\rightarrow 2\omega)$ and then into the fourth-harmonic mode 4ω $(2\omega+2\omega\rightarrow 4\omega)$. We consider the adiabatic limit of the strongly damped fourth-harmonic mode when only modes $\omega,2\omega$ effectively remain in the cavity [see Fig. 1(a)]. In this case this nonlinear system becomes equivalent to a doubly resonant SHG combined with a nonlinear two-photon absorption from the second-harmonic mode.

We note also that although some effects of cascaded nonlinearities were studied a long time ago [10–12], a strong interest in the interaction of two nonlinear processes has emerged within the past few years. For example, combina-

*Also at Yerevan State University, Alex Manookian 1, 375049, Yerevan, Armenia. Electronic address: root@ipr.arminco.com

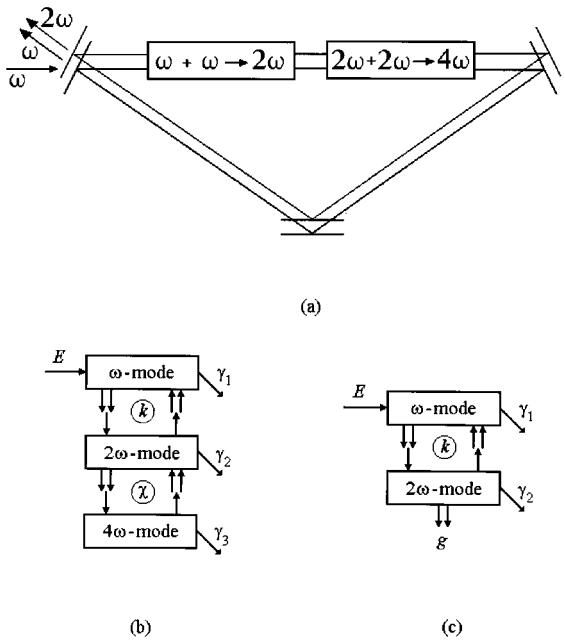

FIG. 1. (a) Principal scheme of the cascaded frequency doubler in the adiabatic regime of generation. (b) Diagrammatic representation of the processes described by the Hamiltonian (1). The boxes represent the intracavity modes at frequencies $\omega_1=\omega$, $\omega_2=2\omega$, and $\omega_3=4\omega$. The arrows correspond to the photons being put into or taken out of the modes (with pairs of arrows denoting pairs of photons) due to the processes of (i) fundamental mode driving (at rate E), (ii) nonlinear transformations (with coupling strengths k and χ), and (iii) damping of the modes (at rates γ_1, γ_2, and γ_3). (c) Diagram representing the adiabatically equivalent model [or the model described by the Hamiltonian (8)], in which the influence of the strongly dumped fourth-harmonic mode is reduced to the two-photon loss mechanism (at the rate $g=\chi/4\gamma_3$) for the second-harmonic mode.

tions of second-order nonlinearities have been investigated in order to induce large $\chi^{(3)}$ nonlinearities [13,14] and to produce tunable UV light [15]. In the context of quantum optics, a scheme with competing processes of SHG and nondegenerate parametric down-conversion has been analyzed with the purpose of generating highly regularized twin beams [16]. Enhanced squeezing from the Kerr interaction combined with two-photon absorption [17] and generation of nonclassical superposition states in a parametric down-conversion combined with two-photon absorption [18,19] have also been predicted. Large quadrature squeezing at high intensities and other specific quantum optical effects have been studied in combinations of $\chi^{(2)}$-nonlinear parametric processes and Kerr interactions [20–22] and for combined processes of four-wave mixing and phase modulation [23,24]. Note that the relevance of these studies goes well beyond the theoretical interests since recent advances in the technology of multiple quantum wells enable practical implementation of some of these complicated devices (see [20] and references therein).

In the nonlinear system under consideration, an important point relevant to the remarkable results is related to the stability properties of the steady states. As it will be shown below, the addition of the second frequency-doubling process or of an equivalent two-photon-absorption mechanism from the second-harmonic mode changes substantially the steady-state behavior of the fundamental and second-harmonic modes as compared to the process of pure SHG. Namely, the self-pulsing instability, arising at a certain critical value of the driving field intensity, vanishes at higher intensities beyond a second critical point and one again arrives at the stable steady-state regime. Moreover, by variation of control parameters of the system one may reduce the instability domain and make it vanishing, arriving at complete quenching of the self-pulsations and at stabilization of the steady states in the entire domain of variation of the driving field intensity. Turning then to the analysis of quantum fluctuations of the modes and taking into account the fact that both the processes of SHG and two-photon absorption are responsible for amplitude squeezing (see, e.g., [4]), one may anticipate capability of our nonlinear system to produce bright light beams with enhanced squeezing properties in the stable steady-state regime.

The paper is organized as follows. In Sec. II we formulate the model of the intracavity cascaded frequency doubler, derive stochastic equations of motion for the three resonant cavity modes, and then eliminating adiabatically the fourth-harmonic mode arrive at a reduced set of equations for the fundamental and second-harmonic modes. This is equivalent to the model of SHG combined with resonant two-photon absorption. In Sec. III we present a semiclassical analysis of the system. We calculate the steady-state solutions and carry out a linear stability analysis, as well as turn to the cavity output intensities of the modes. Section IV is devoted to the analysis of quantum fluctuations of the fundamental and second-harmonic modes within the framework of linearization procedure around the stable steady state. We analyze the intracavity variances of quadrature amplitude fluctuations of the modes and calculate the squeezing spectra of the cavity-output fields. Concluding remarks are given in Sec. V. In the Appendix we derive the equations of motion for the concrete physical system with two crystals and obtain expressions for the coupling constants.

II. MODEL AND STOCHASTIC EQUATIONS OF MOTION

The nonlinear optical interaction under consideration is realized within a triply resonant cavity that supports the modes at frequencies $\omega_1=\omega$, $\omega_2=2\omega$ and $\omega_3=4\omega$, referred to as fundamental, second-harmonic, and fourth-harmonic modes, respectively. The fundamental mode is resonantly driven by an external driving field, while the second- and fourth-harmonic modes are created via cascaded $\chi^{(2)}$-nonlinear processes of frequency doubling (second-harmonic generation). The losses in the input-output cavity mirror are accounted for by means of independent reservoir interactions for each mode. We adopt the following model Hamiltonian, in the rotating-wave approximation:

$$H=\sum_{i=1}^{3}\hbar\omega_i a_i^{\dagger}a_i+i\frac{\hbar k}{2}(a_1^{\dagger 2}a_{2-}-a_1^2a_2^{\dagger})+i\frac{\hbar\chi}{2}(a_2^{\dagger 2}a_3-a_2^2a_3^{\dagger})$$
$$+i\hbar(Ee^{-i\omega t}a_1^{\dagger}-E^{*}e^{i\omega t}a_1)+\sum_{i=1}^{3}(a_i\Gamma_i^{\dagger}+a_i^{\dagger}\Gamma_i), \qquad (1)$$

where $a_i^\dagger$ and a_i $(i=1,2,3)$ are creation and annihilation operators for the modes ω_i, k is the coupling constant for the frequency-doubling process $\omega+\omega\rightarrow 2\omega$ $(\omega_1+\omega_1\rightarrow\omega_2)$, in which two photons of the fundamental mode annihilate to create a photon of the second-harmonic mode, and the χ constant is responsible for the subsequent frequency-doubling process $2\omega+2\omega\rightarrow 4\omega$ $(\omega_2+\omega_2\rightarrow\omega_3)$ creating the photons of the fourth-harmonic mode. E is associated with the coherent driving field amplitude and $\Gamma_i^\dagger,\Gamma_i$ are reservoir operators, giving rise to the cavity damping rates γ_i for the modes ω_i. A diagrammatic representation of the processes described by the Hamiltonian (1) is shown in Fig. 1(b).

We use the standard approach (see, e.g., [25,26]) to eliminate the reservoir operators and to derive the following master equation for the density operator ρ of the modes in the interaction picture:

$$\frac{\partial\rho}{\partial t}=\frac{k}{2}[a_1^{\dagger 2}a_2-a_1^2a_2^\dagger,\rho]+\frac{\chi}{2}[a_2^{\dagger 2}a_3-a_2^2a_3^\dagger,\rho]+[Ea_1^\dagger-E^*a_1,\rho]+\sum_{i=1}^{3}\gamma_i(2a_i\rho a_i^\dagger-\rho a_i^\dagger a_i-a_i^\dagger a_i\rho). \tag{2}$$

The master equation (2) is then transformed into the Fokker-Planck equation in the positive-P representation [25,26,28], which is equivalent to the stochastic differential equations

$$\frac{d\alpha_1}{dt}=-\gamma_1\alpha_1+k\alpha_1^\dagger\alpha_2+E+\Gamma_1(t),$$

$$\frac{d\alpha_2}{dt}=-\gamma_2\alpha_2-\frac{k}{2}\alpha_1^2+\chi\alpha_2^\dagger\alpha_3+\Gamma_2(t), \tag{3}$$

$$\frac{d\alpha_3}{dt}=-\gamma_3\alpha_3-\frac{\chi}{2}\alpha_2^2,$$

where $\Gamma_{1,2}(t)$ are Gaussian noise terms with zero means and nonzero correlators

$$\langle\Gamma_1(t)\Gamma_1(t')\rangle=k\alpha_2\delta(t-t'),$$

$$\langle\Gamma_2(t)\Gamma_2(t')\rangle=\chi\alpha_3\delta(t-t'). \tag{4}$$

We recall that in the positive-P representation used, α_i^+ and α_i are independent complex c-number variables, corresponding to the operators $a_i^\dagger$ and a. The equations for $\alpha_i^\dagger$ variables are obtained from Eq. (3) by exchanging $\alpha_i\leftrightarrow\alpha_i^\dagger$, $\Gamma_{1,2}\rightarrow\Gamma_{1,2}^+$ and term E by its complex conjugate.

It should be noted that the Hamiltonian (1) and Eq. (3) in particular describe the following cascaded scheme of generation with two crystals of different nonlinear susceptibilities placed within a triply resonant ring cavity. We assume for definition that phase-matching conditions for modes ω_1,ω_2 are satisfied in the first crystal and for modes ω_2,ω_3 in the second crystal. In other words, we assume that both of the frequency-doubling processes $\omega_1+\omega_1\rightarrow\omega_2$ and $\omega_2+\omega_2\rightarrow\omega_3$ take place effectively only in the definite nonlinear crystal. In the Appendix we study in detail this point and derive Eqs. (3) and the Hamiltonian (1) on the basis of semiclassical equations of nonlinear optics (see, for example, [29–31]). Such consideration allows us to obtain the following expressions for the coupling constants and damping rates in Eqs. (3):

$$\gamma_i=c\,\frac{1-R_i}{L-L_1-L_2+n_i^{(1)2}L_1+n_i^{(2)2}L_2},$$

$$k=4\pi\hbar^{1/2}\omega_1^{3/2}\chi_1L_1\int_S u_1^2(\rho)u_2^*(\rho)d^2\rho, \tag{5}$$

$$\chi=4\pi\hbar^{1/2}\omega_2^{3/2}\chi_2L_2\int_S u_2^2(\rho)u_3^*(\rho)d^2\rho,$$

where $\chi_1\equiv\chi_1^{(2)}(\omega_2=\omega_1+\omega_1)$, and $\chi_2\equiv\chi_2^{(2)}(\omega_3=\omega_2+\omega_2)$ are nonlinear susceptibilities for each of two crystals, the functions u_i describe the cross-section structure of the modes, R_i is the output reflectivity of the input-output mirror for the ith mode, $n_i^{(j)}$ is the linear susceptibility for the ith mode in the jth crystal, $L_{1,2}$ are the lengths of the crystals, and L is the cavity length.

In what follows we shall consider the limit $\gamma_3\gg\gamma_{1,2}$ of high cavity losses for the fourth-harmonic mode. This allows us to eliminate it adiabatically, using the relation

$$\alpha_3=-\frac{\chi}{2\gamma_3}\alpha_2^2, \tag{6}$$

and to arrive at the following reduced set of equations of motion for the fundamental and second-harmonic modes:

$$\frac{d\alpha_1}{dt}=-\gamma_1\alpha_1+k\alpha_1^\dagger\alpha_2+E+\Gamma_1(t),$$

$$\frac{d\alpha_2}{dt}=-\gamma_2\alpha_2-\frac{k}{2}\alpha_1^2-\frac{\chi^2}{2\gamma_3}\alpha_2^2\alpha_2^\dagger+\Gamma_2(t). \tag{7}$$

Now the nonzero correlators of the noise terms are

$$\langle\Gamma_1(t)\Gamma_1(t')\rangle=k\alpha_2\delta(t-t'),$$

$$\langle\Gamma_2(t)\Gamma_2(t')\rangle=-\frac{\chi^2}{2\gamma_3}\alpha_2^2\delta(t-t'). \tag{8}$$

Model of the frequency doubler combined with two-photon absorption

In the considered limit of the strongly damped fourth-harmonic mode its influence on the dynamics of the second-harmonic mode may be visualized as a nonlinear two-photon-absorption mechanism. Indeed, the set of equations of motion of the form (7) may be directly obtained by considering a combined nonlinear system in which the frequency-doubling process $\omega+\omega\rightarrow 2\omega$ is accompanied by a nonlinear two-photon absorption from the second-harmonic mode $\omega_2=2\omega$. The corresponding effective Hamiltonian may be written as

$$H=\sum_{i=1}^{2}\hbar\omega_i a_i^\dagger a_i+i\frac{\hbar k}{2}(a_1^{\dagger 2}a_2-a_1^2a_2^\dagger)$$
$$+i\hbar(Ee^{-i\omega t}a_1^\dagger-E^*e^{i\omega t}a_1)+\sum_{i=1}^{2}(a_i\Gamma_i^\dagger+a_i^\dagger\Gamma_i)$$
$$+(a_2^2\Gamma^\dagger+a_2^{\dagger 2}\Gamma). \tag{9}$$

Here the first four terms describe the well-known model of intracavity second-harmonic generation [1], while the last term is responsible for the process of two-photon absorption from the second-harmonic mode via a nonlinear nonsaturable absorber [4,32], with $\Gamma^\dagger$ and Γ being the corresponding reservoir operators giving rise to the photon-absorption rate g. The processes described by this Hamiltonian [or by Eqs. (7)] are represented in Fig. 1(c).

Eliminating the reservoir operators $\Gamma_i^\dagger,\Gamma_i$ and $\Gamma^\dagger,\Gamma$, now we arrive at the following master equation for the fundamental and the second-harmonic mode:

$$\frac{\partial\rho}{\partial t}=\frac{k}{2}[a_1^{\dagger 2}a_2-a_1^2a_2^\dagger,\rho]+[Ea_1^\dagger-E^*a_1,\rho]$$
$$+\sum_{i=1}^{2}\gamma_i(2a_i\rho a_i^\dagger-\rho a_i^\dagger a_i-a_i^\dagger a_i\rho)$$
$$+g(2a_2^2\rho a_2^{\dagger 2}-\rho a_2^{\dagger 2}a_2^2-a_2^{\dagger 2}a_2^2\rho). \tag{10}$$

Transforming again to the corresponding Fokker-Planck equation and turning then to the equivalent stochastic equations, we obtain a set of equations of motion, which have the same form and noise properties as Eqs. (7) and (8) with the only difference being that the relation $\chi^2/4\gamma_3$ should be replaced by

$$\frac{\chi^2}{4\gamma_3}\to g. \tag{11}$$

Thus all the results of the subsequent sections can be equally applied to both the nonlinear optical schemes by means of the variable change formula (11).

The physical meaning of the above considerations is related to the fact that the influence of the adiabatically eliminated fourth-harmonic mode is reduced to an additional effective loss mechanism for the second-harmonic mode, which is of two-photon dissipation variety. All the specific results (as compared with those of the well-known model of pure second-harmonic generation [1,4]) discussed below originate actually from this additional two-photon loss mechanism and its stabilizing influence on the nonlinear dynamics of the system.

III. SEMICLASSICAL ANALYSIS

In this section we proceed with the analysis of our nonlinear system in the semiclassical approximation. This is achieved by ignoring the noise terms in Eqs. (7) and by treating the $\alpha_i^\dagger$ variables as complex conjugates to α_i ($\alpha_i^\dagger\to\alpha_i^*$). We calculate in particular the corresponding steady-state solutions and carry out the standard linear stability analysis with respect to small deviations from the steady states.

For this purpose it is more convenient to transform the semiclassical counterpart of Eqs. (7) to the intensity (in photon number units) and phase variables of the modes $\alpha_i=\sqrt{n_i}\exp(i\varphi_i)$. This yields

$$\frac{dn_1}{dt}=-2\gamma_1 n_1+2kn_1\sqrt{n_2}\cos(2\varphi_1-\varphi_2)$$
$$+2|E|\sqrt{n_1}\cos(\phi-\varphi_1),$$
$$\frac{dn_2}{dt}=-2\gamma_2 n_2-kn_1\sqrt{n_2}\cos(2\varphi_1-\varphi_2)-\frac{\chi^2}{\gamma_3}n_2^2,$$
$$\frac{d\varphi_1}{dt}=\frac{|E|}{\sqrt{n_1}}\sin(\phi-\varphi_1)-k\sqrt{n_2}\sin(2\varphi_1-\varphi_2), \tag{12}$$
$$\frac{d\varphi_2}{dt}=-\frac{kn_1}{2\sqrt{n_2}}\sin(2\varphi_1-\varphi_2),$$

where ϕ is a phase of the driving field $E=|E|\exp(i\phi)$.

Then the steady-state solutions ($dn_i/dt=d\varphi_i/dt=0$) for the intensities $n_{1,2}^0$ and phases $\varphi_{1,2}^0$ of the fundamental and the second-harmonic modes are found to satisfy the relations

$$n_1^0=\sqrt{\frac{n_2^0}{K}}(2r+Gn_2^0), \tag{13}$$

$$\varepsilon^2=\sqrt{\frac{n_2^0}{K}}(2r+Gn_2^0)(1+\sqrt{Kn_2^0})^2, \tag{14}$$

$$\varphi_1^0=\phi,\quad \varphi_2^0-2\varphi_1^0=\pi, \tag{15}$$

where we have introduced the dimensionless parameters

$$K\equiv\frac{k^2}{\gamma_1^2},\quad G\equiv\frac{\chi^2}{\gamma_1\gamma_3},\quad r\equiv\frac{\gamma_2}{\gamma_1},\quad \varepsilon^2\equiv\frac{|E|^2}{\gamma_1^2}. \tag{16}$$

To check the stability properties of these steady-state solutions we linearize the equations of motion (12) and write down the equations for small deviations $\delta n_i(t)=n_i(t)-n_i^0$ and $\delta\varphi_i(t)=\varphi_i(t)-\varphi_i^0$ from the steady states in the matrix form

$$\frac{d\delta n}{dt}=-A_n\delta n,\quad \frac{d\delta\varphi}{dt}=-A_\varphi\delta\varphi, \tag{17}$$

where $\delta n=(\delta n_1,\delta n_2)^T$, $\delta\varphi=(\delta\varphi_1,\delta\varphi_2)^T$, and the matrices A_n and A_φ are

$$A_n=\begin{pmatrix}\gamma_1+k\sqrt{n_2^0} & \dfrac{kn_1^0}{\sqrt{n_2^0}}\\ -k\sqrt{n_2^0} & \gamma_2+\dfrac{3\chi^2}{2\gamma_3}n_2^0\end{pmatrix}, \tag{18}$$

$$A_{\varphi}=\begin{pmatrix} \gamma_1-k\sqrt{n_2^0} & k\sqrt{n_2^0} \\ -\dfrac{kn_1^0}{\sqrt{n_2^0}} & \dfrac{kn_1^0}{2\sqrt{n_2^0}} \end{pmatrix}.$$

The steady-state solutions (13) and (14) are stable if the real parts of the eigenvalues of the matrices A_n and A_{φ} are positive. We denote these eigenvalues as $\lambda_{1,2}$ and $\lambda_{3,4}$, respectively, and with use of the notations (16) find

$$\begin{aligned}\lambda_{1,2}=&\frac{\gamma_1}{2}\left(1+r+\sqrt{Kn_2^0}+\frac{3G}{2}n_2^0\right)\\&\pm\frac{\gamma_1}{2}\left[\left(1+r+\sqrt{Kn_2^0}+\frac{3G}{2}n_2^0\right)^2-4Kn_1^0\right.\\&\left.-4(1+\sqrt{Kn_2^0})\left(r+\frac{3G}{2}n_2^0\right)\right]^{1/2},\end{aligned}\tag{19}$$

$$\begin{aligned}\lambda_{3,4}=&\frac{\gamma_1}{2}\left(1-\sqrt{Kn_2^0}+\frac{n_1^0}{2}\sqrt{\frac{K}{n_2^0}}\right)\\&\pm\frac{\gamma_1}{2}\left[\left(1-\sqrt{Kn_2^0}+\frac{n_1^0}{2}\sqrt{\frac{K}{n_2^0}}\right)^2\right.\\&\left.-2Kn_1^0-2n_1^0\sqrt{\frac{K}{n_2^0}}\right]^{1/2}.\end{aligned}$$

A. Self-pulsing instability and stabilization

Using relation (13), one may express the eigenvalues $\lambda_{1,2}$ and $\lambda_{3,4}$ in terms of n_2^0 and check that the real parts of $\lambda_{1,2}$ are always positive, while Re $\lambda_{3,4}$ can take negative values if

$$Y\equiv 1+r+\frac{G}{2}n_2^0-\sqrt{Kn_2^0}<0.\tag{20}$$

Thus the inequality (20) represents the condition for the occurrence of instability in our nonlinear system, which originates from the phase-variable subsystem. This condition is fulfilled for the case

$$\frac{2G(1+r)}{K}<1\tag{21}$$

in the domain

$$n_2^{(-)}<n_2^0<n_2^{(+)},\tag{22}$$

where

$$n_2^{(\pm)}=\frac{K}{G^2}\left[1\pm\sqrt{1-\frac{2G(1+r)}{K}}\right]^2\tag{23}$$

represents the values of n_2^0 at critical Hopf bifurcation points. At these points the real parts of λ_3 and λ_4 vanish, leaving nonzero imaginary parts.

Using the steady-state relation (14), one may express the two critical points in terms of the cavity-input driving field intensity parameter $\varepsilon^2=|E|^2/\gamma_1^2$:

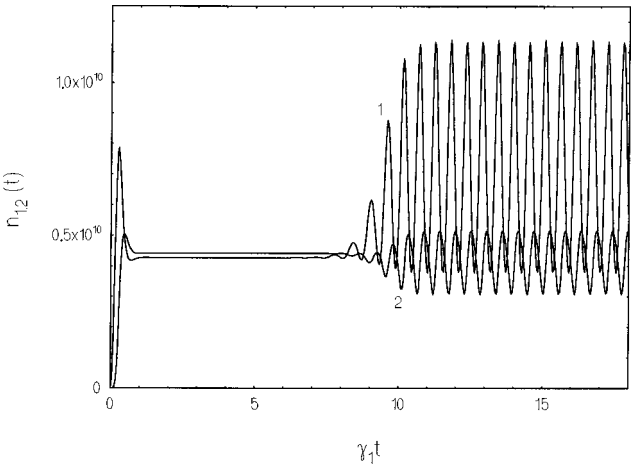

FIG. 2. Self-pulsing instability of the fundamental and second-harmonic mode photon numbers $n_1(t)=|\alpha_1(t)|^2$ (curve 1) and $n_2(t)=|\alpha_2(t)|^2$ (curve 2) as depending on $\gamma_1 t$: $K=10^{-8}$, $G=2.5\times10^{-9}$, $r=1$, $\varepsilon=5\times10^5$, $\alpha_1(0)=1+i$, and $\alpha_2(0)=0$.

$$\begin{aligned}(\varepsilon^{(\pm)})^2=&\frac{1}{G}\left(1\pm\sqrt{1-\frac{2G(1+r)}{K}}\right)\\&\times\left(2r+\frac{K}{G}\left[1\pm\sqrt{1-\frac{2G(1+r)}{K}}\right]^2\right)\\&\times\left(1+\frac{K}{G}\left[1\pm\sqrt{1-\frac{2G(1+r)}{K}}\right]\right)^2.\end{aligned}\tag{24}$$

In the instability domain $(\varepsilon^{(-)})^2<\varepsilon^2<(\varepsilon^{(+)})^2$ the intensities $n_1(t)$ and $n_2(t)$ of the fundamental and the second-harmonic modes demonstrate self-pulsing temporal behavior. This is shown in Fig. 2 by numerical solution of the semiclassical counterpart of Eqs. (7) (i.e., without the noise terms), yielding in particular realizations for $n_1(t)=|\alpha_1(t)|^2$ and $n_2(t)=|\alpha_2(t)|^2$ as depending on the initial conditions $\alpha_1(0)$ and $\alpha_2(0)$.

As for the case

$$\frac{2G(1+r)}{K}>1,\tag{25}$$

the reverse of inequality (21), the quantity Y becomes always positive, leading to positive real parts $\lambda_{3,4}$. As a consequence, in this case we do not observe instability at all, i.e., the steady-state solutions (13)–(15) become stabilized in the entire domain of the driving field intensity parameter ε^2. The relation $2G(1+r)/K=1$ marks the boundary where the two critical points $\varepsilon^{(-)2}$ and $\varepsilon^{(+)2}$ become coincident and the self-pulsing behavior becomes completely quenched.

Let us discuss now in more detail the conditions (25) of stabilization of generated modes. As mentioned previously in Sec. II for equations of motion, the results obtained describe both nonlinear optical schemes. For the model of Sec. II A, in which the frequency-doubling process $\omega_1+\omega_1\rightarrow\omega_2$ is accompanied by two-photon absorption, the intensities and phases of modes can be obtained from the general results by using the variable change formula (11) $G\rightarrow 4g/\gamma_1$. This procedure gives the condition of stability

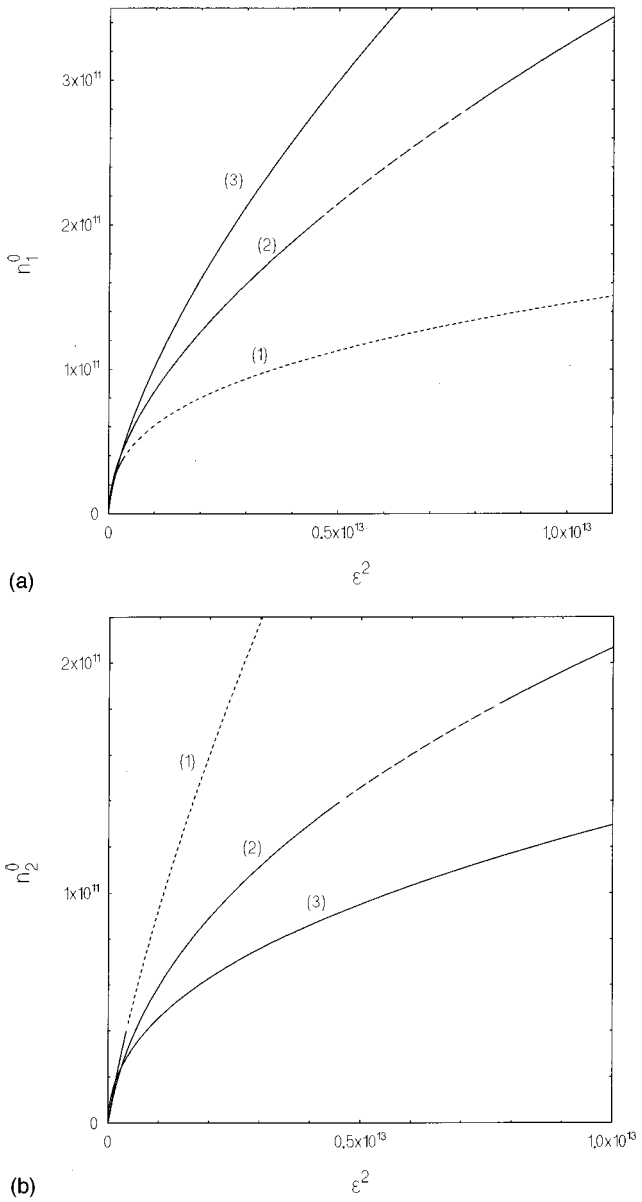

FIG. 3. Semiclassical steady-state photon numbers n_1^0 and n_2^0 for the (a) fundamental and (b) second-harmonic modes as depending on ε^2. The broken parts of the curves are related to the unstable domains: (1) $K=10^{-10}$, $G=0$ (pure SHG), $r=1$; (2) $K=10^{-10}$, $G=2.49\times10^{-11}$, $r=1$; and (3) $K=10^{-10}$, $G=10^{-10}$, $r=0.1$.

$$g \geqslant \frac{k^2}{8(\gamma_1+\gamma_2)}, \tag{26}$$

which can be fulfilled for a sufficiently large rate of the effective two-photon losses. Then, we recall that the cascaded frequency-doubler system is considered here in the adiabatic approximation for $\gamma_3 \gg \gamma_1, \gamma_2$. In this limit the condition of complete stabilization of the steady-state solutions occurs when

$$\frac{\chi^2}{k^2} \geqslant \frac{\gamma_3}{2(\gamma_1+\gamma_2)} \gg 1. \tag{27}$$

In Fig. 3 we plot examples of the curves for the steady-state photon numbers n_1^0 and n_2^0 depending on ε^2. The dashed parts of the curves correspond to the instability domains and the curves for the case of pure SHG are also plotted for comparison. We note that the results on pure SHG can be directly reproduced from our present results by setting $\chi=0$ (or $G=0$). In this case the location of the formally defined second critical point is moved to the infinity so that the system becomes characterized by a single critical point, above which it demonstrates self-pulsing instability. The location of the critical point is determined now by Eq. (20) with $G=0$. Using also relation (14), we arrive at the following well-known results [1] for critical values of n_2^0 and ε in the process of SHG:

$$n_2^{cr}=\frac{(\gamma_1+\gamma_2)^2}{k^2}, \quad \varepsilon^{cr}=\frac{(2\gamma_1+\gamma_2)}{k\gamma_1}[2\gamma_2(\gamma_1+\gamma_2)]^{1/2}. \tag{28}$$

Curves (3) on Figs. 3(a) and 3(b) describe the examples of complete stabilized behavior of the photon numbers, which is realized for the parameters $G=K$ and the ratio of the coupling constants $\chi^2/k^2=\gamma_3/\gamma_1 \gg 1$. This quality can be written in terms of the nonlinear susceptibilities of two combined crystals $\chi_1/\chi_2=2\sqrt{2\gamma_1/\gamma_3}L_2/L_1$ if we use Eqs. (5) and neglect the cross-section structure of the modes. If we choose $\gamma_3/\gamma_1 \approx 200$ (according to the adiabatic approximation), then $\chi_1/\chi_2=L_2/5L_1$, which is a quite acceptable situation for real physical systems.

Thus the inclusion of an additional two-photon loss mechanism into the model of SHG changes substantially the stability properties of the resulting nonlinear system. It becomes characterized [in the case of Eq. (21)] by two critical points and hence by a finite instability domain, above which the steady states become again stable. Moreover, when the two-photon loss efficiency becomes strong enough to yield the inequalities (25)–(27), we do not observe any critical point or instability. Another obvious influence of the effective two-photon losses from the second-harmonic mode consists in a decrease of the magnitude of n_2^0 as compared to the case of pure SHG [see Fig. 3 curve (2)].

B. Cavity-output intensities

We consider the special scheme of generation when the coupling in and out fields occur at one of the ring-cavity mirrors. To calculate the intensities of the cavity-output intensities at the fundamental and second-harmonic mode frequencies in this case we use the well-known relation [32]

$$a_i^{out}=\sqrt{2\gamma_i}a_i-a_i^{in} \quad (i=1,2), \tag{29}$$

which expresses the cavity-output field operators (a_i^{out}) in terms of the intracavity (a_i) and cavity-input (a_i^{in}) operators.

The cavity-output intensities in photon number units per unit time are determined by $n_i^{out}=\langle (a_i^{out})^\dagger a_i^{out}\rangle$. Taking into account that only the fundamental mode is coherently driven by an external field with $\langle a_1^{in}\rangle=E/\sqrt{2\gamma_1}[n_1^{in}=\langle (a_1^{in})^\dagger a_1^{in}\rangle = |E|^2/2\gamma_1]$, while the second-harmonic mode is initially in the vacuum state $[\langle a_2^{in}\rangle=\langle (a_2^{in})^\dagger a_2^{in}\rangle=0]$, we obtain for n_i^{out}, in the steady-state regime and in the semiclassical approximation $[\langle a_i\rangle=\sqrt{n_i^0}\exp(i\varphi_i^0), \quad \langle a_i^\dagger a_i\rangle=n_i^0]$,

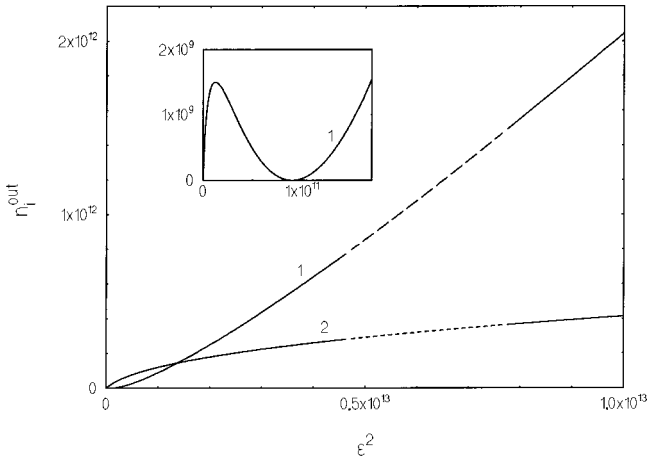

FIG. 4. Scaled cavity-output intensities $n_{1,2}^{out}/\gamma_1$ of the (1) fundamental and (2) second-harmonic modes as depending on ε^2 for $K=10^{-10}$, $G=2.49\times10^{-11}$, and $r=1$.

$$n_1^{out}=2\gamma_1\left(\sqrt{n_1^0}-\frac{|E|}{2\gamma_1}\right)^2, \tag{30}$$

$$n_2^{out}=2\gamma_2 n_2^0. \tag{31}$$

With the use of Eqs. (13) and (14), the quantities $n_{1,2}^{out}$ may be expressed in terms of the cavity-input field intensity $n_1^{in}=|E|^2/2\gamma_1=\gamma_1\varepsilon^2/2$. Examples of the curves for scaled output intensities n_1^{out}/γ_1 and n_2^{out}/γ_1 depending on the scaled input intensity $2n_1^{in}/\gamma_1=\varepsilon^2$ are plotted in Fig. 4. A closeup view, showing the complete depletion of the fundamental beam, i.e., vanishing of n_1^{out} at a certain value of ε^2, is also shown in Fig. 4.

In Fig. 5 we plot the coefficient

$$\eta=\frac{\omega_2 n_2^{out}}{\omega_1 n_1^{in}}=\frac{2n_2^{out}}{n_1^{in}} \tag{32}$$

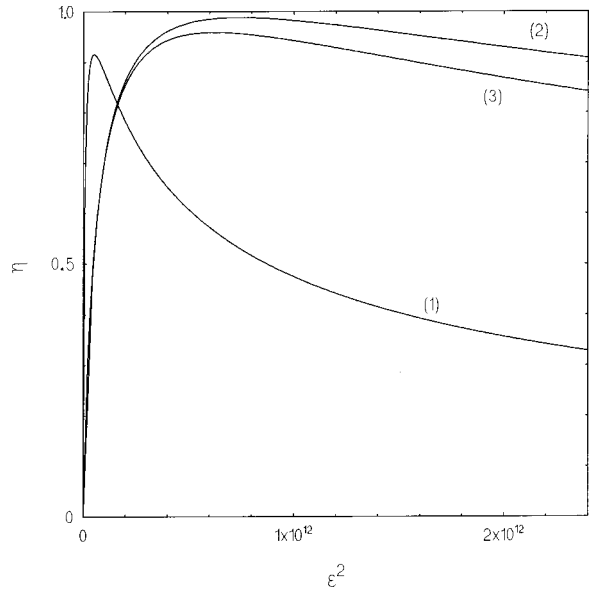

FIG. 5. Dependence of the coefficient η on ε^2 for (1) $K=10^{-10}$, $G=2.49\times10^{-11}$, $r=1$; (2) $K=10^{-10}$, $G=2.49\times10^{-11}$, $r=10$; and (3) $K=10^{-10}$, $G=10^{-10}$, $r=10$.

of energy transformation from the cavity-input fundamental beam to the cavity-output second-harmonic beam depending on ε^2. The fact that the maximal value of the η coefficient does not approach unity due to the depletion of the fundamental beam is caused by the two-photon loss mechanism from the second-harmonic mode.

IV. QUANTUM FLUCTUATIONS AND QUADRATURE SQUEEZING

Let us turn now to the analysis of quantum fluctuations of the fundamental and second-harmonic modes. We carry out this analysis within the framework of standard linearized treatment of quantum fluctuations (around the semiclassical steady states), which is valid in the stability domains of the nonlinear system.

In accordance with the results of the preceding section, an attractive property of our nonlinear system consists in the stabilization of the steady states at high intensities of the modes. This leads to the validity of the results of the linearized theory at high intensities and motivates the study, in particular, the quantum fluctuations of the quadrature amplitudes of the high-intensity light beams. The purpose is to obtain bright light with enhanced quadrature squeezing properties in the stable generation regime. Our reasoning for such an expectation relates to the origin on the restriction on squeezing results, obtainable for the process of pure SHG [4]. These restrictions originate from the fact that although the quadrature amplitude fluctuations of the modes decrease monotonically with an increase of the corresponding intensities, the results of the linearized theory become invalid at high intensities in the above critical region. As a consequence, the minimal variance of the quadrature amplitude fluctuations (maximal squeezing) and the corresponding maximal intensity turn out to be bounded, in the stable regime, by their values at the critical point.

The linearized equations of motion for our nonlinear system, which contain the noise terms and describe the quantum fluctuations of the intensities and phases of the modes, can be derived from Eqs. (7) and (8) by transforming to the new stochastic variables

$$n_i=\alpha_i^\dagger\alpha_i, \quad \varphi_i=\frac{1}{2i}\ln\frac{\alpha_i}{\alpha_i^\dagger}. \tag{33}$$

Using then the same notations for fluctuations $\delta n_i(t)=n_i(t)-n_i^0$ and $\delta\varphi_i(t)=\varphi_i(t)-\varphi_i^0$ as in the semiclassical equation (17), one may arrive at following linearized equations:

$$\frac{d}{dt}\begin{pmatrix}\delta n_1\\ \delta n_2\end{pmatrix}=-A_n\begin{pmatrix}\delta n_1\\ \delta n_2\end{pmatrix}+\begin{pmatrix}F_1(t)\\ F_2(t)\end{pmatrix}, \tag{34}$$

$$\frac{d}{dt}\begin{pmatrix}\delta\varphi_1\\ \delta\varphi_2\end{pmatrix}=-A_\varphi\begin{pmatrix}\delta\varphi_1\\ \delta\varphi_2\end{pmatrix}+\begin{pmatrix}f_1(t)\\ f_2(t)\end{pmatrix}, \tag{35}$$

where matrices A_n and A_φ are given by Eq. (18) and the nonzero correlators of the noise terms $F_i(t)$ and $f_i(t)$ are

$$\langle F_1(t)F_1(t')\rangle=-2kn_1^0\sqrt{n_2^0}\,\delta(t-t'),$$

$$\langle F_2(t)F_2(t')\rangle = -\frac{\chi^2}{\gamma_3}(n_2^0)^2\delta(t-t'), \tag{36}$$

$$\langle f_1(t)f_1(t')\rangle = \frac{k\sqrt{n_2^0}}{2n_1^0}\delta(t-t'),$$

$$\langle f_2(t)f_2(t')\rangle = \frac{\chi^2}{4\gamma_3}\delta(t-t'). \tag{37}$$

A. Intracavity variances

To study the squeezing properties of the fundamental and second-harmonic modes we calculate first the corresponding intracavity variances

$$V_i(\theta_i) = \langle[\Delta X_i(\theta_i)]^2\rangle = \langle[X_i(\theta_i)]^2\rangle - \langle X_i(\theta_i)\rangle^2 \quad (i=1,2) \tag{38}$$

of the rotated quadrature phase amplitude operators $X_i(\theta_i) = a^\dagger\exp(i\theta_i) + a\exp(-i\theta_i)$, with θ_i being the phases of the local oscillators. The variance $V_i(\theta_i)$ may be expressed in terms of the correlators $\langle\delta n_i^2\rangle$ and $\langle\delta\varphi_i^2\rangle$ [23], which are calculated with the use of the solutions of Eqs. (34) and (35) and of the correlators (36) and (37). Due to the negativity of the noise correlators (36) of the intensity variable subsystem, the squeezing effect $[V_i(\theta_i)<1]$ is realized for the case $\theta_i = \varphi_i^0$, i.e., for amplitude fluctuations of the modes. The final results for the variances $V_i(\theta_i=\varphi_i^0)\equiv V_i$ take the form

$$V_1 = 1 + \frac{\langle\delta n_1^2\rangle}{n_1^0} = 1 - \frac{GKn_1^0n_2^0 + 2\sqrt{Kn_2^0}[Kn_1^0 + (r+\frac{3}{2}Gn_2^0)(1+r+\frac{3}{2}Gn_2^0+\sqrt{Kn_2^0})]}{2[1+r+\frac{3}{2}Gn_2^0+\sqrt{Kn_2^0}][Kn_1^0+(1+\sqrt{Kn_2^0})(r+\frac{3}{2}Gn_2^0)]}, \tag{39}$$

$$V_2 = 1 + \frac{\langle\delta n_2^2\rangle}{n_2^0} = 1 - \frac{2Kn_1^0\sqrt{Kn_2^0} + Gn_2^0[Kn_1^0+(1+\sqrt{Kn_2^0})(1+r+\frac{3}{2}Gn_2^0+\sqrt{Kn_2^0})]}{2[1+r+\frac{3}{2}Gn_2^0+\sqrt{Kn_2^0}][Kn_1^0+(1+\sqrt{Kn_2^0})(r+\frac{3}{2}Gn_2^0)]}. \tag{40}$$

Using Eqs. (13) and (14) for n_1^0 and n_2^0, the results (39) and (40) may be expressed in terms of the driving field intensity parameter ε^2. Examples of the curves for V_1 and V_2 depending on ε^2 are represented in Fig. 6 for different values of parameters K, G, and r. The curves relating to the pure SHG ($G=0$) are also given for comparison. The broken parts of the curves relate to the instability domains, where the linearized treatment of quantum fluctuations fails. We see that both the variances V_1 and V_2 demonstrate substantial noise reduction in the below- and above-instability domains, as well as in the case of complete stabilization of the steady state (full curves). The squeezing effect is greater than in the case of pure SHG and an essential property is that the squeezing is realized at higher intensities of the modes. This implies that our nonlinear system is capable of generation bright light beams with enhanced squeezing properties.

B. Cavity-output squeezing spectra

When discussing the squeezing properties of a mode of radiation field, one needs to take into account that an appropriate experimentally measurable quantity is related to the squeezing spectrum for the cavity-output field [4]. Using the standard definition, we calculate the squeezing spectra of the cavity-output fields at the fundamental and second-harmonic mode frequencies, corresponding to the amplitude fluctuations [23]

$$S_i(\omega) = 1 + \frac{2\gamma_i}{n_i^0}\langle\delta n_i(-\omega)\,\delta n_i(\omega)\rangle \quad (i=1,2). \tag{41}$$

The unity on the right-hand side of Eq. (41) corresponds to the shot-noise level and the squeezed noise reduction is realized when $S_i(\omega)<1$. The spectral correlators $\langle\delta n_i(-\omega)\,\delta n_i(\omega)\rangle$ may be calculated with the use of the Fourier transform of Eqs. (34) and (36), yielding

$$S_1(\omega) = 1 - \frac{1}{d(\omega)}\left\{4\sqrt{Kn_2^0}\left[\left(r+\frac{3}{2}Gn_2^0\right)^2 + \left(\frac{\omega}{\gamma_1}\right)^2\right] + 2KGn_1^0n_2^0\right\}, \tag{42}$$

$$S_2(\omega) = 1 - \frac{1}{d(\omega)}\left\{2rGn_2^0\left[(1+\sqrt{Kn_2^0})^2 + \left(\frac{\omega}{\gamma_1}\right)^2\right] + 4Krn_1^0\sqrt{Kn_2^0}\right\}, \tag{43}$$

where

$$d(\omega) = \left[(1+\sqrt{Kn_2^0})(r+\tfrac{3}{2}Gn_2^0) + Kn_1^0 - \left(\frac{\omega}{\gamma_1}\right)^2\right]^2 + \left(\frac{\omega}{\gamma_1}\right)^2[1+r+\tfrac{3}{2}Gn_2^0+\sqrt{Kn_2^{0\,2}}]. \tag{44}$$

Examples of the squeezing spectra $S_1(\omega)$ and $S_2(\omega)$ are represented in Fig. 7 for different values of parameters K, G, r, and ε^2. For small values of ε^2, the spectra have one minimum at zero frequency, while with increasing ε^2 we have divisions into two minima at sideband frequencies. In Fig. 8 we plot the dependence of the minimal values $S_i(\omega_{opt})$ at the optimal frequency as depending on ε^2. The squeezing effect in the fundamental mode is increased with a decrease of the relation $r=\gamma_2/\gamma_1$ and it is increased in the case $r\gg 1$ for the second-harmonic mode.

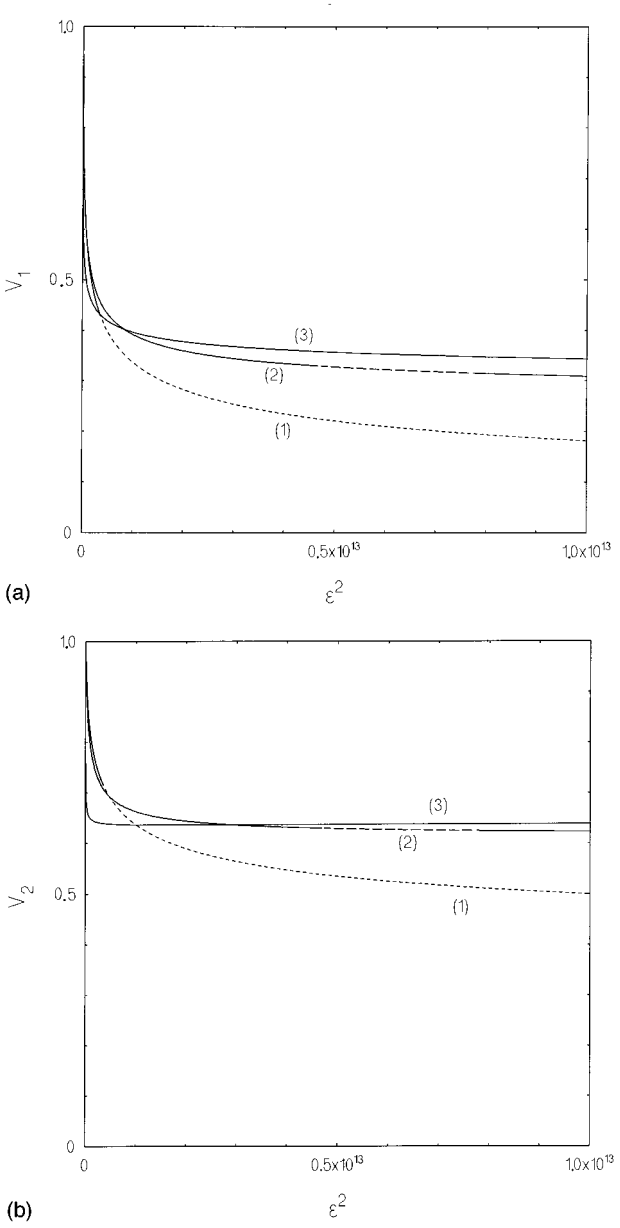

FIG. 6. Quadrature amplitude variances V_i for the (a) fundamental and (b) second-harmonic modes as depending on ε^2: (1) $K=10^{-10}$, $G=0$ (pure SHG), $r=1$; (2) $K=10^{-10}$, $G=2.49\times10^{-11}$, $r=1$; and (3) $K=10^{-10}$, $G=10^{-10}$, $r=0.1$.

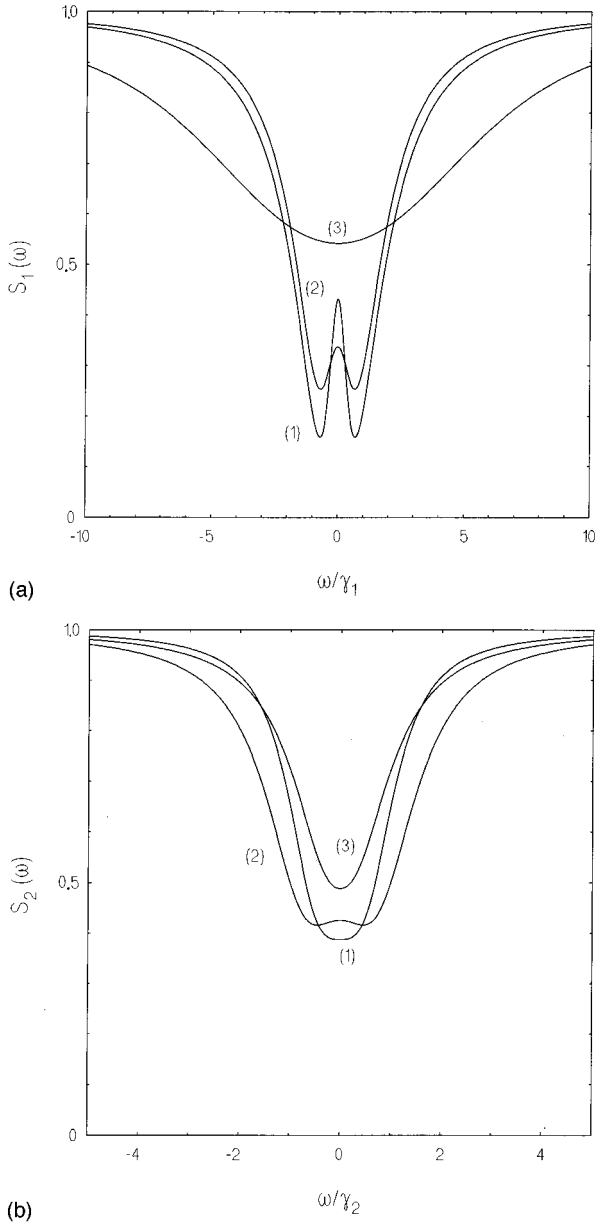

FIG. 7. Squeezing spectra $S_i(\omega)$ of the (a) fundamental and (b) second-harmonic modes as depending on ω/γ_i: (a) $K=10^{-10}$, $G=2.49\times10^{-11}$, $r=0.1$, $\varepsilon^2=7.5\times10^9$ [curve (1)]; $K=10^{-10}$, $G=10^{-10}$, $r=0.1$, $\varepsilon^2=8.24\times10^9$ [curve (2)]; and $K=10^{-10}$, $G=10^{-10}$, $r=0.1$, $\varepsilon^2=1.8\times10^9$ [curve (3)]. (b) $K=10^{-10}$, $G=2.49\times10^{-11}$, $r=10$, $\varepsilon^2=0.62\times10^{13}$ [curve (1)]; $K=10^{-10}$, $G=2.49\times10^{-11}$, $r=10$, $\varepsilon^2=1.97\times10^{13}$ [curve (2)]; and $K=10^{-10}$, $G=10^{-10}$, $r=10$, $\varepsilon^2=0.24\times10^{13}$ [curve (3)].

An interesting peculiarity of the squeezing properties of our nonlinear system is that, in contrast to a number of previously studied nonlinear optical interactions [4], the maximal squeezing is not approached at the critical point of the system. When comparing our squeezing results with those for the process of pure SHG, we also arrive at the following conclusion. The maximal degree of squeezing achievable in our system at a particular frequency does not exceed the squeezing in pure SHG. However, a moderate degree of squeezing still remains achievable when turning to higher intensities of the modes and to the integral characteristics of the squeezing spectra. We recall that the integral squeezing is related to the intracavity variance V_i

$$\frac{1}{2\pi}\int_{-\infty}^{\infty} d\omega[S_i(\omega)-1]=2\gamma_i(V_i-1). \tag{45}$$

Using this relation and the results of Sec. IV A, one may conclude that the enhanced squeezing at a high level of coherent excitation is related to the broadening of the spectral range where the noise reduction effect is substantial. In other words, our results indicate the possibility of production of high-intensity broadband squeezed-light beams.

V. CONCLUSION

In conclusion, we have presented a semiclassical and quantum analysis of a model of an intracavity cascaded fre-

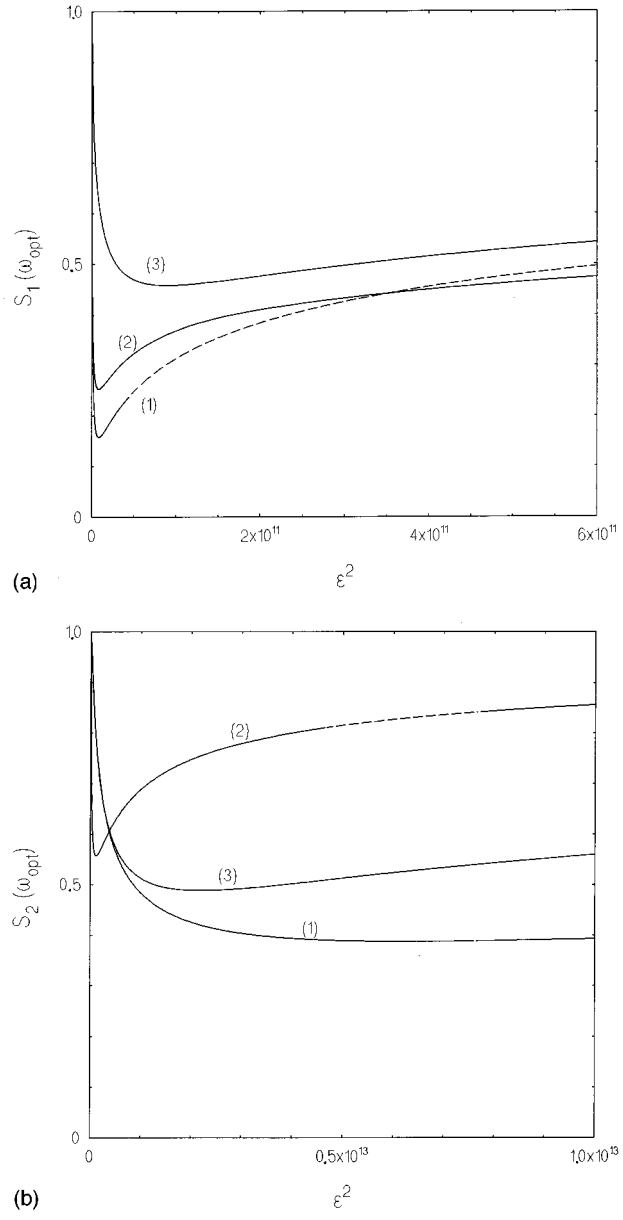

FIG. 8. Dependence of the minimal values $S_i(\omega_{opt})$ of the squeezing spectra at the optimal frequencies on ε^2: (a) fundamental mode with $K=10^{-10}$, $G=2.49\times10^{-11}$, $r=0.1$ [curve (1)]; $K=10^{-10}$, $G=10^{-10}$, $r=0.1$ [curve (2)]; and $K=10^{-10}$, $G=2.49\times10^{-11}$, $r=1$ [curve (3)] and (b) second-harmonic mode with $K=10^{-10}$, $G=2.49\times10^{-11}$, $r=10$ [curve (1)]; $K=10^{-10}$, $G=2.49\times10^{-11}$, $r=1$ [curve (2)]; and $K=10^{-10}$, $G=10^{-10}$, $r=10$ [curve (3)].

quency doubler, in which an externally driven fundamental mode at frequency ω transforms subsequently into the second- and fourth-harmonic modes ($\omega+\omega\rightarrow2\omega$ and $2\omega+2\omega\rightarrow4\omega$). In the adiabatic limit of the strongly damped fourth-harmonic mode, the model becomes equivalent to the process of intracavity SHG combined with two-photon absorption from the generated second-harmonic mode.

The final results, written in a general form, are equally applied to both models. The inclusion of an additional frequency-doubling process or an equivalent two-photon loss mechanism from the second-harmonic mode influences strongly the nonlinear dynamics and stability properties of the nonlinear system as compared to the process of pure SHG. The system under consideration demonstrates two critical points and a finite instability domain: The semiclassical steady-state solutions are stable in two domains, below the first critical point and beyond the second critical point at higher pump intensities. Moreover, when the rate of the effective two-photon losses exceeds some critical value [see Eqs. (25)–(27)], the instability domain vanishes and we observe completed stabilization of the steady-state behavior of the system. In terms of the $\chi^{(2)}$-nonlinear coupling constants k and χ, which are responsible, respectively, for the first and second frequency-doubling processes, the complete stabilization occurs when $\chi^2/k^2\sim\gamma_3/\gamma_1\gg1$, or, more exactly, when the conditions (26) and (27) are valid. As shown, our analyses (Sec. III A) of these conditions can be fulfilled for real physical systems containing two crystals with different nonlinear susceptibilities χ_1 and χ_2 [see Fig. 1(a)]. For example, the crystal KH_2PO_4 gives $\chi_1\approx0.245\times10^{-12}$ m/V for $\lambda_1=1.06$ μm and KD_2PO_4 gives $\chi_2\approx0.25\times10^{-12}$ m/V for $\lambda_2=0.53$ μm. In this case and for other parameters $R_1=R_2=99.5\%$, $R_3=15\%$, $L_1\approx0.9$ cm, $L_2\approx2$ cm, $L=30$ cm and spot size 0.47 mm, we have $K=10^{-10}$, $G=2.49\times10^{-11}$, $r=1$, which lead to regimes shown in Fig. 3, curves (2). If the cavity-input field power is $P_{in}=\hbar\omega_1\gamma_1\varepsilon^{(-)2}/2=2.3$ W at the first critical point we have $P_{out}^{(1)}=0.785$ W and $P_{out}^{(2)}=0.54$ W for the fundamental and the second-harmonic modes. For $P_{in}=3.45$ W, at the second critical point we obtain $P_{out}^{(1)}=1.3$ W and $P_{out}^{(2)}=0.665$ W.

However, the chosen parameters are not the only ones for this optical scheme. As mentioned above, the obtained results, including those for critical points, intensities [Eqs. (23) and (24)], and squeezing spectra [Eqs. (42) and (43)], are expressed by means of dimensionless values: K,G,r,ε. That is why the dimensionless values, used in Figs. 2–8 can also be realized for other crystals and reflectivities of cavity R_1,R_2,R_3. In particular, for cavities with high reflectivities (see [27]) the critical points may be achieved at lower intensities of the driving field.

For the crystal $Gd_2(MoO_4)_3$, $\chi_1\approx0.025\times10^{-12}$ m/V at $\lambda_1=1.08$ μm and for $K_2C_4H_4O_6\cdot\frac{1}{2}H_2O$, $\chi_2\approx0.06\times10^{-12}$ m/V at $\lambda_2=0.54$ μm, for other parameters $R_1=R_2=99.96\%$, $R_3=90\%$, $L_1=L_2\approx1$ cm, $L=10$ cm, and spot size of 1 mm we have the same parameters $K=10^{-10}$, $G=2.49\times10^{-11}$, and $r=1$. In this case the first critical point was achieved at $P_{in}=0.42$ W and we have $P_{out}^{(1)}=0.14$ W and $P_{out}^{(2)}=0.1$ W for the fundamental and the second-harmonic modes. The second critical point was achieved at $P_{in}=0.7$ W and we have $P_{out}^{(1)}=0.27$ W and $P_{out}^{(2)}=0.13$ W. In the presence of instability, the temporal behavior of the fundamental and second-harmonic mode intensities is of well-known self-pulsing character.

The stability properties of our nonlinear system are reflected also in the quantum analysis carried out within the linearized treatment of quantum fluctuations. The peculiarities of the corresponding results on quadrature amplitude squeezing are caused by the fact that the linearized calculations are applicable not only for relatively small or moderate intensities of the modes in the below-instability domain but also at higher intensities in the above-instability domain. The

results of the calculation of the intracavity variances and cavity-output squeezing spectra of the fundamental and second-harmonic modes demonstrate that the nonlinear system is capable of generating bright amplitude-squeezed light with enhanced noise-reduction properties.

Although the maximal degree of squeezing in the cavity-output beams, which is approached at a particular frequency, is of the same order as in the case of pure SHG, the noise reduction at higher intensities remains substantial if we look for integral characteristics of the squeezing spectra. The squeezed noise reduction is realized now in a wide spectral range. In other words, the cavity-output fields demonstrate a broadband squeezing with high coherent excitation.

ACKNOWLEDGMENT

G.Yu.K. is indebted to Professor S. Fauve for valuable discussions and appreciates hospitality while at Ecole Normale Superieure de Lyon.

APPENDIX

In this appendix we derive the equations of motion (3) and the interaction Hamiltonian (1) for the intracavity modes at frequencies $\omega,2\omega,4\omega$. We consider the scheme of generation with two $\chi^{(2)}$-nonlinear crystals placed one directly after another within a triply resonant ring cavity.

The nonlinear polarization amplitude in the medium is

$$\mathbf{P}=\chi^{(2)}:\mathbf{EE}, \tag{A1}$$

where $\chi^{(2)}$ is a third-rank susceptibility tensor. We express the electric fields in the cavity as

$$E^{(j)}=\sum_i A_i^{(j)}(l,t)\exp(-i\omega_i t+ik_i^{(j)}l)+\text{c.c.}, \tag{A2}$$

where $i=1,2,3$ correspond to the $\omega,2\omega,4\omega$ modes, $E^{(1,2)}$ are the electric fields in the first and second crystals, respectively, and $E^{(0)}$ in vacuum, $k_i^{(j)}=\omega_i n_i^{(j)}/c$ is the wave vector, and $n_i^{(j)}$ is the linear susceptibility for the ith mode in jth crystal.

Let us derive the equations of motion (3). The classical wave equations in the slowly varying envelope approximation [30,31] read

$$cn_1^{(j)}\frac{\partial A_1^{(j)}}{\partial l}+n_1^{(j)2}\frac{\partial A_1^{(j)}}{\partial t}=2\pi i\omega_1\chi_j^{(2)}(\omega_1=\omega_2-\omega_1)A_2^{(j)}A_1^{(j)*}\exp(i\Delta_{21}^{(j)}l),$$

$$cn_2^{(j)}\frac{\partial A_2^{(j)}}{\partial l}+n_2^{(j)2}\frac{\partial A_2^{(j)}}{\partial t}=2\pi i\omega_2\chi_j^{(2)}(\omega_2=\omega_1+\omega_1)A_1^{(j)2}\exp(-i\Delta_{21}^{(j)}l)$$

$$+2\pi i\omega_2\chi_j^{(2)}(\omega_2=\omega_3-\omega_2)A_3^{(j)}A_2^{(j)*}\exp(i\Delta_{32}^{(j)}l), \tag{A3}$$

$$cn_3^{(j)}\frac{\partial A_3^{(j)}}{\partial l}+n_3^{(j)2}\frac{\partial A_3^{(j)}}{\partial t}=2\pi i\omega_3\chi_j^{(2)}(\omega_3=\omega_2+\omega_2)A_2^{(j)2}\exp(-i\Delta_{32}^{(j)}l)$$

in crystals $(j=1,2)$ and

$$c\frac{\partial A_i^{(0)}}{\partial l}+\frac{\partial A_i^{(0)}}{\partial t}=0,$$

in vacuum, where $i=1,2,3$, and $\Delta_{nm}^{(j)}=k_n^{(j)}-2k_m^{(j)}$. Neglecting the reflection waves from the crystals' faces we write down the following boundary conditions for the mode amplitudes:

$$A_i^{(1)}(l_1,t)=A_i^{(0)}(l_1,t)\exp[il_1(k_i^{(0)}-k_i^{(1)})],$$

$$A_i^{(0)}(l_1+L_1,t)=A_i^{(1)}(l_1+L_1,t)\exp[i(l_1+L_1)(k_i^{(1)}-k_i^{(0)})],$$

$$A_i^{(2)}(l_2,t)=A_i^{(0)}(l_2,t)\exp[il_2(k_i^{(0)}-k_i^{(2)})], \tag{A4}$$

$$A_i^{(0)}(l_2+L_2,t)=A_i^{(2)}(l_2+L_2,t)\exp[i(l_2+L_2)(k_i^{(2)}-k_i^{(0)})],$$

$$A_i^{(0)}(0,t)=R_iA_i^{(0)}(L,t)\exp(ik_i^{(0)}L)+A_i^{dr},$$

where $l_{1,2}$ are the coordinates of crystals' entrances, $L_{1,2}$ are the lengths of crystals, L is the cavity length, R_i is the output reflectivity of input or output mirror for the ith mode, and A_i^{dr} are the amplitudes of driving fields.

Assume the amplitudes of all the modes vary slowly along the crystals' length. Then we can state they are independent from the path variable l in all Eqs. (A3), in addition to the terms $\partial/\partial l$. Using the conditions (A4) we define

$$A_i^{(0)}\equiv A_i, \quad l\in[0,l_1]$$

$$A_i^{(1)}=A_i\exp[il_1(k_i^{(0)}-k_i^{(1)})], \quad l\in[l_1,l_1+L_1]$$

$$A_i^{(0)}=A_i\exp[iL_1(k_i^{(1)}-k_i^{(0)})], \quad l\in[l_1+L_1,l_2],$$

$$A_i^{(2)}=A_i\exp[iL_1(k_i^{(1)}-k_i^{(0)})+il_2(k_i^{(0)}-k_i^{(2)})], \tag{A5}$$

$$l\in[l_2,l_2+L_2]$$

$$A_i^{(0)}=A_i\exp[iL_1(k_i^{(1)}-k_i^{(0)})+iL_2(k_i^{(2)}-k_i^{(0)})],$$

$$l\in[l_2+L_2,L].$$

Then substituting Eq. (A5) into Eqs. (A3) and taking integral over the cavity length, we obtain using the boundary conditions (A4)

$$(L-L_1-L_2+n_1^{(1)2}L_1+n_1^{(2)2}L_2)\,\frac{\partial A_1}{\partial t}=-c(1-R_1\exp i\Phi_1)A_1+cA_1^{dr}$$
$$+2\pi\omega_1\chi_1^{(2)}(\omega_1=\omega_2-\omega_1)A_2A_1^*[\exp(i\Delta_{21}^{(1)}L_1)-1]/\Delta_{21}^{(1)}$$
$$+2\pi\omega_1\chi_2^{(2)}(\omega_1=\omega_2-\omega_1)A_2A_1^*\exp(i\Delta_{21}^{(1)}L_1)[\exp(i\Delta_{21}^{(2)}L_2)-1]/\Delta_{21}^{(2)},$$

$$(L-L_1-L_2+n_2^{(1)2}L_1+n_2^{(2)2}L_2)\,\frac{\partial A_2}{\partial t}=-c(1-R_2\exp i\Phi_2)A_2$$
$$+2\pi\omega_2\chi_1^{(2)}(\omega_2=\omega_1+\omega_1)A_1^2[1-\exp(-i\Delta_{21}^{(1)}L_1)]/\Delta_{21}^{(1)}$$
$$+2\pi\omega_2\chi_1^{(2)}(\omega_2=\omega_3-\omega_2)A_3A_2^*[\exp(i\Delta_{32}^{(1)}L_1)-1]/\Delta_{32}^{(1)}$$
$$+2\pi\omega_2\chi_2^{(2)}(\omega_2=\omega_1+\omega_1)A_1^2\exp(-i\Delta_{21}^{(1)}L_1)[1-\exp(-i\Delta_{21}^{(2)}L_2)]/\Delta_{21}^{(2)}$$
$$+2\pi\omega_2\chi_2^{(2)}(\omega_2=\omega_3-\omega_2)A_3A_2^*\exp(i\Delta_{32}^{(1)}L_1)[\exp(i\Delta_{32}^{(2)}L_2)-1]/\Delta_{32}^{(2)}, \tag{A6}$$

$$(L-L_1-L_2+n_3^{(1)2}L_1+n_3^{(2)2}L_2)\,\frac{\partial A_3}{\partial t}=-c(1-R_3\exp i\Phi_3)A_3$$
$$+2\pi\omega_3\chi_1^{(2)}(\omega_3=\omega_2+\omega_2)A_2^2[1-\exp(-i\Delta_{32}^{(1)}L_1)]/\Delta_{32}^{(1)}$$
$$+2\pi\omega_3\chi_2^{(2)}(\omega_3=\omega_2+\omega_2)A_2^2\exp(-i\Delta_{32}^{(1)}L_1)[1-\exp(-i\Delta_{32}^{(2)}L_2)]/\Delta_{32}^{(2)},$$

where we assume $n_i^{(j)}\approx 1$ in the terms with $\partial/\partial l$ and we use the definition $\Phi_i\equiv k_i^{(0)}(L-L_1-L_2)+k_i^{(1)}L_1+k_i^{(2)}L_2$.

We suppose the validity of conditions

$$\Phi_i=2\pi N_i, \tag{A7}$$

where N_i are some integer numbers, which define the wave vectors and assume that the phase-matching conditions for the modes $\omega,2\omega$ are satisfied in the first crystal and for the modes $2\omega,4\omega$ in the second crystal. These conditions are

$$2k_1^{(1)}=k_2^{(1)}\quad(\Delta_{21}^{(1)}=0),$$
$$2k_2^{(2)}=k_3^{(2)}\quad(\Delta_{32}^{(2)}=0). \tag{A8}$$

In addition, we use also the equalities

$$\Delta_{32}^{(1)}L_1=2\pi N_1,\quad \Delta_{21}^{(2)}L_2=2\pi N_2, \tag{A9}$$

which are a consequence of Eqs. (A7) and (A8). On the whole we obtain

$$(L-L_1-L_2+n_1^{(1)2}L_1+n_1^{(2)2}L_2)\,\frac{\partial A_1}{\partial t}=-c(1-R_1)A_1+cA_1^{dr}+2\pi i\omega_1\chi_1^{(2)}(\omega_1=\omega_2-\omega_1)A_2A_1^*L_1,$$

$$(L-L_1-L_2+n_2^{(1)2}L_1+n_2^{(2)2}L_2)\,\frac{\partial A_2}{\partial t}=-c(1-R_2)A_2+2\pi i\omega_2\chi_1^{(2)}(\omega_2=\omega_1+\omega_1)A_1^2L_1$$
$$+2\pi i\omega_2\chi_2^{(2)}(\omega_2=\omega_3-\omega_2)A_3A_2^*L_2, \tag{A10}$$

$$(L-L_1-L_2+n_3^{(1)2}L_1+n_3^{(2)2}L_2)\,\frac{\partial A_3}{\partial t}=-c(1-R_3)A_3+2\pi i\omega_3\chi_2^{(2)}(\omega_3=\omega_2+\omega_2)A_2^2L_2.$$

We express then the amplitudes A_i in the form [28]

$$A_i=i\sqrt{\frac{\hbar\omega_i}{2\varepsilon_0}}\,u_i(\rho)\alpha_i, \tag{A11}$$

where $u_i(\rho)$ $(i=1,2,3)$ define the beams cross-section structure and satisfy the normalization conditions

$$[L-L_1-L_2+n_i^{(1)2}L_1+n_i^{(2)2}L_2]\int_S u_i(\rho)u_i^*(\rho)d^2\rho=1,$$
$$i=1,2,3. \tag{A12}$$

Substituting Eq. (A11) into Eqs. (A10) and taking into account the condition of normalization (A12) and the relations

$$\chi_j^{(2)}(\omega_1=\omega_2-\omega_1)=2\chi_j^{(2)}(\omega_2=\omega_1+\omega_1),$$

$$\chi_j^{(2)}(\omega_2=\omega_3-\omega_2)=2\chi_j^{(2)}(\omega_3=\omega_2+\omega_2)$$

(see [29]), we integrate over the cross section and then obtain Eq. (3) in a semiclassical approximation

$$\frac{\partial\alpha_1}{\partial t}=-\gamma_1\alpha_1+E+k\alpha_1^*\alpha_2,$$

$$\frac{\partial\alpha_2}{\partial t}=-\gamma_2\alpha_2-\frac{k}{2}\alpha_1^2+\chi\alpha_2^*\alpha_3, \qquad \text{(A13)}$$

$$\frac{\partial\alpha_3}{\partial t}=-\gamma_3\alpha_3-\frac{\chi}{2}\alpha_2^2,$$

where the coefficients are given by Eq. (5).

Let us now derive the interaction Hamiltonian (1). The Hamiltonian is defined as [29]

$$H=:\int d^3\mathbf{r}\left(\frac{\mathbf{B}^2}{2\mu_0}+\frac{\varepsilon_0\mathbf{E}^2}{2}+\frac{4\pi}{3}\chi^{(2)}\mathbf{E}^3\right):, \qquad \text{(A14)}$$

where :: denotes normal ordering. Using Eqs. (A7)–(A9) and (A12), it is easily proved that expression (A14) leads to the Hamiltonian (1) without the part of the reservoir.

[1] P. D. Drummond, K. J. McNeil, and D. F. Walls, Opt. Acta **27**, 321 (1980); **28**, 211 (1981).

[2] H. J. Kimble and J. L. Hall, in *Quantum Optics IV*, edited by J. D. Harvey and D. F. Walls (Springer, Berlin, 1986).

[3] L. Lugiato, G. Strini, and F. de Martini, Opt. Lett. **8**, 256 (1983).

[4] M. J. Collett and D. F. Walls, Phys. Rev. A **32**, 2887 (1985).

[5] S. F. Pereira, M. Xiao, H. J. Kimble, and J. L. Hall, Phys. Rev. A **38**, 4931 (1988).

[6] A. Sizmann, R. J. Horowicz, G. Wagner, and G. Leuchs, Opt. Commun. **80**, 138 (1990).

[7] P. Kürtz, R. Paschotta, K. Fiedler, A. Sizmann, G. Leuchs, and J. Mlynek, Appl. Phys. B: Photophys. Laser Chem. **55**, 216 (1992); P. Kürtz, R. Paschotta, K. Fiedler, A. Sizmann, and J. Mlynek, Europhys. Lett. **24**, 449 (1993).

[8] R. Paschotta, M. J. Collett, P. Kürtz, K. Fiedler, H. A. Bacor, and J. Mlynek, Phys. Rev. Lett. **72**, 3807 (1994).

[9] N. P. Pettiaux, P. Mandel, and C. Fabre, Phys. Rev. Lett. **66**, 1838 (1991).

[10] J. A. Armstrong, N. Bloembergen, J. Ducuing, and P. S. Pershan, Phys. Rev. **127**, 1918 (1962).

[11] J.-M. R. Thomas and J.-P. E. Taran, Opt. Commun. **4**, 329 (1972).

[12] D. N. Klyshko and B. F. Polkovnikov, Sov. J. Quantum Electron. **3**, 324 (1974).

[13] R. De Salvo, D. J. Hagan, M. Sheik-Bahae, G. Stegeman, E. W. Van Stryland, and H. Vanheerzeele, Opt. Lett. **17**, 28 (1992); R. De Salvo, M. Sheik-Bahae, A. A. Said, D. J. Hagan, and E. W. Van Stryland, *ibid.* **18**, 194 (1993).

[14] D. Y. Kim, W. E. Torruellas, J. Kang, C. Bosshard, G. I. Stegeman, P. Vidakovic, J. Zyss, W. E. Moerner, R. Twieg, and G. Bjorklund, Opt. Lett. **19**, 868 (1994); S. Nitti, H. M. Tan, G. P. Banfi, and V. Degorgio, Opt. Commun. **106**, 263 (1994); R. Danielius, P. Di Trapani, A. Dubiatis, A. Piskarskas, D. Podenas, and G. P. Banfi, Opt. Lett. **18**, 574 (1993).

[15] G. T. Moore, K. Koch, and E. C. Cheung, Opt. Commun. **113**, 463 (1995).

[16] M. A. M. Marte, Phys. Rev. Lett. **74**, 4815 (1995); J. Opt. Soc. Am. B **12**, 2296 (1995).

[17] C. C. Gerry and E. E. Hach III, Opt. Commun. **100**, 211 (1993).

[18] C. C. Gerry and E. E. Hach III, Phys. Lett. A **174**, 185 (1993).

[19] L. Gilles, B. M. Garraway, and P. L. Knight, Phys. Rev. A **49**, 2785 (1994).

[20] C. Cabrillo and F. J. Bermejo, Phys. Rev. A **48**, 2433 (1993).

[21] G. Yu. Kryuchkyan and K. V. Kheruntsyan, Opt. Commun. **127**, 230 (1996).

[22] K. V. Kheruntsyan, D. S. Krähmer, G. Yu. Kryuchkyan, and K. G. Petrossian, Opt. Commun. **139**, 157 (1997).

[23] G. Yu. Kryuchkyan and K. V. Kheruntsyan, Quantum Semiclassic. Opt. **7**, 529 (1995); JETP **83**, 875 (1996).

[24] G. Yu. Kryuchkyan *et al.*, Quantum Opt. **7**, 965 (1995).

[25] D. F. Walls and G. J. Milburn, *Quantum Optics* (Springer, Berlin, 1994).

[26] P. D. Drummond and C. W. Gardiner, J. Phys. A **13**, 2353 (1980).

[27] Z. Y. Ou, S. F. Pereira, E. S. Polzik, and H. J. Kimble, Opt. Lett. **17**, 640 (1992).

[28] P. D. Drummond and D. F. Walls, J. Phys. A **13**, 725 (1980).

[29] N. Bloembergen, *Nonlinear Optics* (Benjamin, New York, 1965).

[30] Y. R. Shen, *The Principles of Nonlinear Optics* (Wiley, New York, 1984).

[31] A. Yariv, *Optical Waves in Crystals* (Wiley, New York, 1984).

[32] M. J. Collett and C. W. Gardiner, Phys. Rev. A **30**, 1386 (1984).